INTERFACE

royalsocietypublishing.org/journal/rsif

Research

Cite this article: Matherne M, Dowell-Esquivel C, Howington O, Lenaghan O, Steinbach G, Yunker PJ, Hu DL. 2021 Biomechanics of pollen pellet removal by the honey bee. *J. R. Soc. Interface* **18**: 20210549.
https://doi.org/10.1098/rsif.2021.0549

Received: 30 June 2021
Accepted: 2 August 2021

Subject Category:
Life Sciences–Physics interface

Subject Areas:
biomaterials, biomechanics, biophysics

Keywords:
pollen, pollination, honey bee, viscoelastic

Author for correspondence:
David L. Hu
e-mail: hu@me.gatech.edu

Electronic supplementary material is available online at https://doi.org/10.6084/m9.figshare.c.5557413.

THE ROYAL SOCIETY
PUBLISHING

Biomechanics of pollen pellet removal by the honey bee

Marguerite Matherne[1], Caroline Dowell-Esquivel[2], Oliver Howington[5], Olivia Lenaghan[1], Gabi Steinbach[3], Peter J. Yunker[3] and David L. Hu[1,4]

[1]School of Mechanical Engineering, [2]School of Biomedical Engineering, [3]School of Physics, and [4]School of Biology, Georgia Institute of Technology, Atlanta, GA 30332, USA
[5]School of Biology, University of North Georgia, Oakwood, GA 30566, USA

DLH, 0000-0002-0017-7303

Honey bees (*Apis mellifera*) carry pollen back to their hive by mixing it with nectar and forming it into a pellet. The pellet must be firmly attached to their legs during flight, but also easily removable when deposited in the hive. How does the honey bee achieve these contrary aims? In this experimental study, we film honey bees removing pollen pellets and find they peel them off at speeds 2–10 times slower than their typical grooming speeds. Using a self-built pollen scraper, we find that slow removal speeds reduce the force and work required to remove the pellet under shear stress. Creep tests on individual pollen pellets revealed that pollen pellets are viscoelastic materials characterized by a Maxwell model with long relaxation times. The relaxation time enables the pellet to remain a solid during both transport and removal. We hope that this work inspires further research into viscoelastic materials in nature.

1. Introduction

Biological adhesion and attachment mechanisms, from octopus tentacles [1] to ant feet [2], have long pushed the envelope for speed, strength and reversibility [3]. Conversely, the ability to detach is also vital to many organisms' ability to locomote, groom and perform other similar behaviours [4]. As such, most studies of detachment focus on removing an appendage from a substrate [4]. In this study, we consider how the honey bee removes its pollen pellet, which it intentionally adheres to its legs. We show how the viscoelastic properties of the pollen pellet facilitate both safe transport and removal. In nature, many liquids produced by organisms are viscoelastic, such as the slime produced by the hagfish [5,6] and the mucus of terrestrial snails and slugs [7]. Understanding how nature manipulates viscoelastic materials may inspire new ways to manufacture and manipulate soft materials [8].

Honey bees are the most economically valuable pollinators, and with 35% of the world's crop production depending on pollinators [9], understanding how honey bees interact with pollen is important to maintaining our food supply. Pollen is the main source of protein in a honey bee's diet and the primary food for their brood [10]. To collect and transport pollen, honey bees mix it with regurgitated nectar and form it into a pellet, an example of which is shown in figure 1*a*. They carry the pellet on their hind (metathoracic) legs in a structure called the corbicula, or pollen basket, which is shown in figure 1*b*–*d*. Previous research has shown that a colony will collect 10–26 kg of pollen per year [10]. While the weights of a honey bee's pollen pellets vary with the time of day and with the species of pollen, the average pollen pellet weighs 7.9 mg [11], with the honey bee carrying two pollen pellets, one on each hind leg. This means that an average colony will annually embark on up to 1.6 million foraging trips to collect up to 3.2 million pollen pellets to support colony survival. Clearly the process of attachment and detachment of the pollen pellet must be highly reliable for such pollen collection to occur in such high numbers.

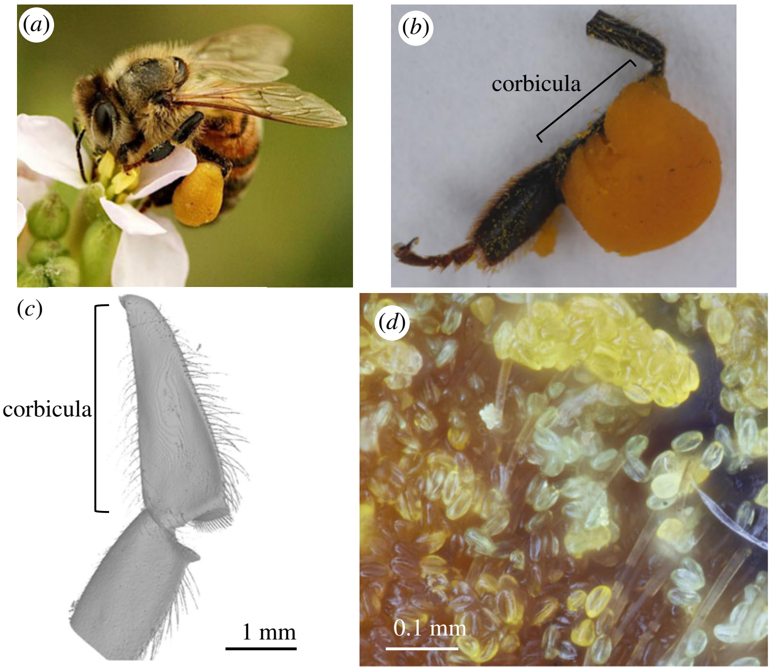

Figure 1. The honey bee collecting pollen. (*a*) A honey bee on a flower with a pollen pellet in its corbicula. Image credit to Avi ben zaken, used under license CC BY-SA. (*b*) A close up of a pollen pellet on an excised honey bee hind leg. The corbicula is the part of the leg underneath the pollen pellet. (*c*) A microCT scan of a honey bee's hind leg. The top segment is the corbicula, which is fringed with long, curved hairs. (*d*) A close-up of the corbicular hairs embedded into the pollen pellet. The dark area in the top right indicates a portion of the honey bee's leg, the bright yellow particles are pollen, and the hairs are the translucent cylinders extending from the leg into the pollen pellet. Image by Marguerite Matherne and Xinjing Xu.

The corbicula, which has an average surface area of 1.81 ± 0.04 mm^2 [12], is a slightly concave, hairless plate surrounded on both sides by long setae, or hairs, that curve inwards, as shown in figure 1*c*. The corbicular hairs are attached to nerves and some of them can detect their angle of displacement, which signals to the bee the pollen pellet's size [13]. In the process of forming the pollen pellet, the hairs, at least at the top of the corbicula, become embedded into the pellet, as shown in figure 1*d*. In addition to the outer hairs, there is also a single spindle hair located just above the pollen press, and previous studies have found that this hair plays some role in the maximum possible volume of the pellet [14].

When the honey bee has finished foraging, it returns to the hive and selects a cell in which to deposit its pollen pellets. While the behaviour of the honey bee and other bee species has been reported in great detail [15,16], the behaviour during pellet removal has been described in considerably less detail [17,18]. The only detailed description of how a honey bee removes pollen in the hive that we could find was by Casteel [15]. Beyond this description, the mechanics behind the process has never been investigated. In our study, we measure the kinematics of this process. We rationalize these observations using a combination of force measurement and measurement of rheological properties of the pellet.

2. Methods

2.1. Imaging the pollen pellet and corbicula

The honey bee's hind leg, including the corbicula, was imaged with a DSLR camera (Canon 1D) as shown in figure 1*b* and a microCT scanner (Scanco microCT50) as shown in figure 1*c*. The close-ups of the pollen pellet–corbicula interface in figure 1*d* were captured using a BK PLUS lab system by Dun, Inc. with a 20x microscope objective on a Canon DSLR camera.

2.2. Observing live bees

We filmed honey bees depositing their pollen loads into individual worker cells in August of 2019. Both worker and drone cell types are oriented upwards at a 13° angle [19] to the horizontal to ensure that the content of the cells do not fall out due to gravity. In a Langstroth hive gaps between frames are only 2.2 cm and the colony interior is dark, making filming challenging. To get around these issues, we initially attempted to film a glass observation hive but this only allowed a dorsal view, which did not give access to the bee's leg movement.

To obtain a lateral view, we removed individual frames from the hive. We selected frames that had both cells with freshly deposited pollen and cells with uncapped brood. The presence of fresh pollen suggested that the honey bees had already chosen this as a suitable area to deposit their pollen. The presence of uncapped brood would encourage the bees to deposit their pollen into a nearby cell [17].

Once the frame was chosen, we gently brushed off the honey bees and placed the frame on a surface with one side of the comb facing up. The frame was placed at least 10 feet away from any other hives to ensure no other bees would land on our apparatus. We were able to leave the exposed frame in the same general area as other colonies because we filmed during a nectar flow in late summer mornings on sunny days. This procedure minimized potential robbing behaviour from nearby colonies [20]. We used an aspirator (BioQuip 1135P, Rancho Dominguez, CA, USA) to collect returning pollen foragers at the hive entrance from which the frame was taken. When we had 15–20 honey bees in the aspirator collecting tube, we returned to the removed frame and opened one end of the tube. The bees left the tube and some flew away, but many walked onto the frame. We followed their progress with a video camera (Sony Handycam HDR-XR200V). When a bee inserted its head and front (prothoracic) legs into a cell and inspected it, we trained the camera on it and waited for it to deposit the pollen. Using this method over two summers, we obtained nearly 30 videos, out of which only three had a resolution and filming angle sufficient for us to analyse the removal process.

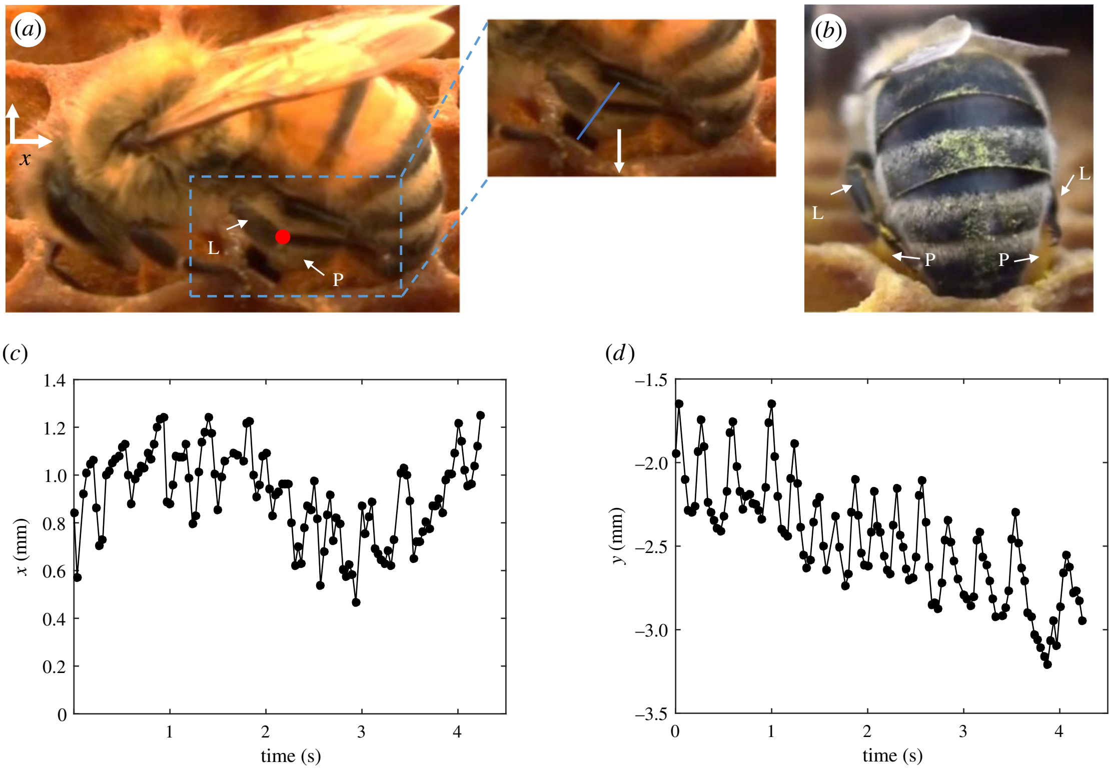

Figure 2. Filming bees deposit pollen in the hive. (*a*,*b*) Honey bees removing pollen pellets and depositing them into beeswax cells from (*a*) a lateral viewpoint and (*b*) a posterior viewpoint. The red mark in (*a*) shows where on the middle leg kinematic data were tracked. The white coordinate axis denotes the point where the *x*–*y* coordinate axes were fixed to account for camera motion. In (*a*,*b*), arrows L point to the middle leg of the bee that pushes off the pollen pellet, and arrow P points to the pollen pellet. The inset of (*a*) shows a close-up of the position of the middle leg during removal. The blue solid line shows the angle of the corbicula, and the white arrow shows the direction the pellet falls during removal. The middle leg peeled off the pollen pellet at an acute angle with respect to the corbicula. (*c*,*d*) Movement of the honey bee's middle leg while removing a pollen pellet in the *x* and *y* directions from the video referenced in (*a*).

Tracker Video Analysis and Modeling Tool software (https://physlets.org/tracker/) was used to track the motion of the bee's middle leg from the joint connecting the tibia (upper segment) and tarsus (lower segment) of the middle (mesothoracic) leg [21], as shown in figure 2*a*. The videos were filmed by hand and afterward digitally stabilized using Apple iMovie. Additionally, the cartesian coordinates were fixed in Tracker to an arbitrary point on the comb so that the tracking data would not be affected by the residual camera motion.

2.3. Measuring the force and work to remove a pollen pellet

To measure the force to remove a pollen pellet, we designed an automated pollen scraper, shown in figure 3*a*, to mimic the behaviour of the bee. We used an aspirator to catch honey bees carrying pollen at the entrance of their hives in Atlanta, GA, USA in October and November 2020. The bees were brought back to the laboratory and anaesthetized by placing them in a freezer at 0°C or lower for 5–10 min. Once unconscious, they were removed from the freezer and their hind legs, laden with pollen pellets, were carefully excised using microscissors (FST item no. 15024-10). The bees were then returned to the freezer before regaining consciousness and were left there for at least 24 h to ensure they did not regain consciousness.

UV curable adhesive (Loctite 4311) was used to glue the posterior side of the excised leg to a rectangle made from plastic scrap. This rectangle facilitated manipulation and placement of the leg. Care was taken to avoid gluing the pollen pellet. The rectangle was attached with tape to a sample holder, composed of a corner bracket taped to a microscope slide, which was in turn placed on an analytical balance (Mettler Toledo XS105), as shown in the inset of figure 3*a*. A servo motor (HiTec HS-625MG), controlled by an Arduino Uno, was attached to a two-bar linkage that drove an artificial bee leg downward at speeds of 0.76, 2.5 or 5 $\mathrm{mm\ s^{-1}}$. The artificial leg, which simulates a bee's middle leg, is comprised of a 0.05 mm diameter rod made from the tip of a medical syringe with the sharp point removed. A honey bee's leg [22] is 0.3 mm in diameter, with additional hair that is 0.25 mm long, which is wider in diameter than the rod used in our experiments. However, when a larger rod was used in the experiment, it was nearly impossible to line the rod and pellet up so that the rod would not come into contact with the leg. Thus, a smaller rod was chosen to remove the pellet.

Initial tests showed difficulty in aligning the artificial leg with the pollen pellet. To ameliorate this problem, a 30 by 5 cm rectangular, laser-cut piece of acrylic was used as a spacer to align the bee leg with the removal arm. The spacer ensured that the arm consistently came into contact with the top of the pollen pellet, rather than the leg. The spacer was removed prior to beginning the test.

As the rod pushed the pellet off of the leg, the resistance force was recorded 10 times per second by the Mettler Toledo analytical balance's software, BalanceLink. A digital USB microscope (Andonstar A1) simultaneously filmed the removal from the side. After the pellet was removed, it was weighed on the analytical balance and its mass recorded. This set-up and the process of removing the pellet can be seen in figure 3*a*,*b* and in electronic supplementary material, video S1.

The work to remove the pellet was calculated by syncing the force data obtained from the analytical balance and the video of the removal. The motion of the artificial leg was tracked to find the relationship between force and displacement. To determine the work done, the area under this curve was calculated in MATLAB using the trapz function. All p-values used to compare means of force and work were calculated using a two-tailed t-test with unequal variance in Microsoft Excel. The averages were considered statistically significant if $p \leq 0.05$.

2.4. Measuring the mechanical properties of the pellet

The mechanical properties of a pollen pellet were measured using a Zwick Roell Universal Testing Machine (UTM). Honey bees carrying pollen pellets were caught at the hive in Atlanta, GA, USA in October 2020. The bees were put into a freezer for 5–10 min until they were unconscious, after which the pellets were then carefully pushed off the leg with a pair of tweezers. Each pellet was placed on a glass microscope slide, oriented so the small axis of the pellet was facing up and was imaged from above using a digital microscope (Andonstar A1). From these images, ImageJ was used to calculate the cross-sectional area of each pellet, which in turn was used to calculate the stress applied by the UTM. All UTM tests were completed within 3 h of catching the bees to reduce the effects of dehydration.

The pollen pellets were subjected to a creep test in the UTM at approach speeds of the compression plate of either 0.1, 0.5, 1 or 2 mm s^{-1} until the target force of 20 mN was reached. Afterwards, the force was held constant and we measured the strain response for 120 s. The value 20 mN was chosen as the target force because the force to remove the pellet described in §2.3 was approximately 20 mN at the speed bees remove pellets, and because that force elicited a small strain, a necessary condition for the Maxwell model [23].

The tests at 2 mm s^{-1} have a sample size of only $N = 2$; this speed approached the limits of what the UTM can measure. This test was attempted approximately 10 times, and only two of those trials did not result in an error message from the UTM.

2.4.1. The Maxwell model

A material is viscoelastic if it exhibits both viscous and elastic behaviour under stress [24]. In other words, it shows both solid and fluid responses to an applied stress. The fluid and solid responses cannot be attributed to a certain material component. For example, the solid response is not necessarily only due to the presence of the pollen particles, and the liquid response is not only due to the presence of the nectar. Instead the material as a whole exhibits both solid and fluid responses. If a pollen pellet is viscoelastic, the speed at which the bee removes it will define the mechanical behaviour the pellet exhibits.

The Maxwell model of viscoelasticity was used to determine the mechanical properties of the pollen pellets based on the UTM tests. The model predicts the behaviour of the material by modelling it as a dash-pot in series with a spring [23]. The spring represents the solid behaviour and its stiffness is Young's modulus E, given by the slope of the stress versus strain curve, $\sigma = E\varepsilon$ where σ is stress and ε is strain. The dash-pot represents the fluid behaviour and is modelled as a piston–cylinder assembly filled with a fluid of viscosity η, where $\dot{\varepsilon} = \sigma/\eta$ and $\dot{\varepsilon}$ is the strain rate, or the derivative of strain with respect to time. The constitutive equation for the Maxwell model is

$$\sigma + \frac{\eta}{E}\dot{\sigma} = \eta\dot{\varepsilon}. \tag{2.1}$$

During a creep test, the applied stress is constant, σ_0, so that $\dot{\sigma} = 0$. Initially when the stress is applied, the spring bears all the stress because it takes time for the dash-pot to react to the stress. Thus, Young's modulus E is the slope of stress versus strain curve when the stress is being applied, i.e. before σ_0 is reached. An example of how E was calculated is shown in electronic supplementary material, figure S4(b). There is an initial condition of the strain of $\varepsilon(t = 0) = \sigma_0/E$.

Using the initial condition and applied stress constraint, equation (2.1) becomes

$$\varepsilon(t) = \sigma_0\left(\frac{1}{\eta}t + \frac{1}{E}\right), \tag{2.2}$$

where t is time. Equation (2.2) may be used to find the viscosity, η, of the pellet by isolating the strain versus time data that corresponds to when the constant stress is applied. The constant stress was determined as the point when the stress reaches 99% of the final stress measured. The average σ_0 and standard deviation for each sample is given in electronic supplementary material, table S1. The stress was not the same for each sample because the UTM holds a set force value and the pellets varied in size. Stress was calculated as the applied force divided by the cross-sectional area of the pellet, as described previously. An example of the isolated constant stress data and the corresponding strain data are shown in electronic supplementary material, figure S4(c,d). The slope of the linear fit of the corresponding strain versus time data is σ_0/η, as shown in electronic supplementary material, figure S4(d).

3. Results

3.1. Honey bees removing pellets in the hive

In summer 2018 and summer 2019, through numerous attempts, we obtained four videos of honey bees removing their pollen pellets. Electronic supplementary material, videos S2 and S3 show a honey bee depositing its pollen pellets into the comb. The honey bee first braces its front legs on the outside of the hexagonal cell. It then presses the feet of its hind legs against the inside of the cell. It uses its middle legs to push the pollen pellet off of the corbicula of the hind legs, moving the middle legs in a back and forth, saw-like motion until the pollen falls off of the corbicula and into the cell. The bee does this simultaneously to both of its pollen pellets. During removal, the middle leg is oriented at an acute angle with respect to the corbicula, as shown in figure 2*a*. That is, the middle leg does not apply stress in a purely normal or purely parallel movement. Rather, as shown in electronic supplementary material, video S2, it exhibits more complex behaviour. The result is that the pellet appears to peel off of the corbicula.

On average, it took the honey bee $T = 2.6 \pm 1.1$ s ($N = 4$) to remove the pollen pellets. The average length of a honey bee's corbicula is $L = 3.16 \pm 0.047$ mm, as estimated from the average of 20 previous measurements from each of 19 different colonies by Milne [12]. The leg length yields an average removal speed of $U = L/T = 1.2 \pm 0.5$ mm s^{-1}.

We obtain further detail on the removal speed by taking into account the oscillatory movement of the middle leg. Having various estimates for the pellet removal speed are especially important to characterize viscoelastic materials, which behave differently depending on shear rate. One video (electronic supplementary material, video S2) captured the entire removal process from an angle that clearly displayed the trajectory of the middle leg (figure 2*a*). The middle leg performs 13–15 periodic sawing motions during the duration of the removal process, as can be seen in the time course of the leg position in the x- and y-directions (horizontal and vertical directions) in figure 2*c*,*d*. The frequencies in the x- and y-directions were 4.0 ± 1.6 Hz and 4.1 ± 1.2 Hz, respectively. In the y-direction, there is an overall downward trend, showing that the honey bee is moving its middle leg

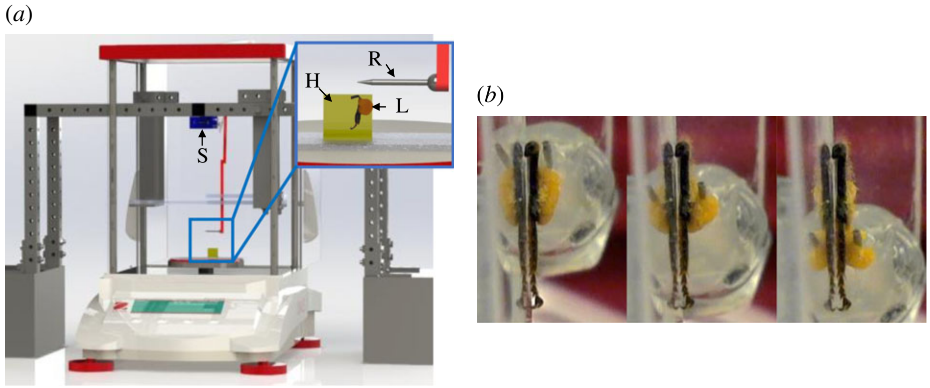

Figure 3. Automated pollen scraper (*a*) Overview of the set-up to measure the force to remove the pollen pellet. The steel frame holds the incoming removal rod without contacting the analytical balance. Inset shows close up of the sample holder and bee leg. S denotes the servo motor, L the bee leg, H the sample holder, and R the removal rod which simulates the scraping motion of the bee. (*b*) Time lapse of a pollen pellet being removed from the leg by the arm. Images are separated by 4 s.

down as it progresses in removing the pellet from the corbicula. Although the previously reported speed U represents the average removal speed from start to finish, we can also consider the speed the leg is moving during the oscillation. We measured the leg's speed during each downward movement in figure 2*c*,*d*. The average speed of the middle leg during the oscillations is $U_x = 2.1 \pm 0.82$ mm s^{-1} in the horizontal (x-direction) and $U_y = 3.9 \pm 1.4$ mm s^{-1} in the vertical (y-direction).

How does the pellet removal speed U compare to the maximum speeds that bees can move their legs? Using 23 time segments of three individual bees grooming pollen from a previous study [22], we find the middle leg has a maximum grooming speed of $U_{\mathrm{groom}} = 11$ mm s^{-1}, a median speed of 4.0 mm s^{-1} and average speed of 4.5 mm s^{-1}. The maximum speed U_{groom} is double the speed of the vertical oscillation U_y, and 10 times the average removal speed U.

3.2. Force to remove a pellet

As noted in the previous section, the bee applies stress to the pellets at an acute angle. This behaviour is difficult to recreate exactly in the lab, so we design experiments to investigate the behaviour of the pollen pellets under two classic types of applied stress: shear and compression. The automated pollen scraper (§2.3) was designed to investigate the behaviour of the pellet when a shear stress is applied.

To understand why the bee's pellet removal speed is so much slower than its grooming, we move the scraper at speeds $U_{\mathrm{mimic}} = 0.76$, 2.5 or 5 mm s^{-1}. The lowest value is comparable to the bee's average removal speed U, and the upper value is comparable to the oscillation speed U_y. However in the following section, we will focus on results for the lower speed because the automated pollen scraper moves in a linear fashion, not in an oscillatory manner like the honey bee's middle leg during pellet removal.

The relationship between the peak pollen removal force and scraper speed are shown in figure 4*a* and table 1. The closed symbols show averages and the error bars represent 95% confidence intervals. Examples of force–time and force–displacement relationships at each speed are shown in figure 4*c*,*d*, with the complete data set in electronic supplementary material, figures S1–S3. In some instances, the measured force does not return to zero at the end of the time series because the pellet remained attached to leg even after the scraper was clear of the corbicula. Also, the total displacement of the scraper depended on the size of the pollen pellet, with small displacements for smaller pellets. Very large pellets extended over the top of the corbicula, giving a displacement longer than the corbicula length.

An important difference between our automated pollen scraper experiments and its biological counterpart is the totality of the pellet removal. In the videos of the bees in the hive and through observations of bees caught at the hive, there is little residue left on the corbicula once the pellet is removed. That is, the bee is able to remove the pellet cleanly and as a whole. The automated pollen scraper often fractured the pellet and left a good amount of residue on the corbicula, as shown in figure 5*b* and table 1.

At the most biologically relevant scraping speed of 0.76 mm s^{-1}, the 95% confidence intervals in figure 5*c*,*d* show that neither the peak force nor the work done depends on whether or not residue was left. At the high speed of 5.0 mm s^{-1}, the average force and work done were both significantly higher in trials that left residue. Fracture can occur in viscoelastic materials at both high and low stresses if the stress is applied over enough time [25]. Therefore, the force to remove the pellets at the low speed of 0.76 mm s^{-1} may not depend on whether or not residue was left because the time elapsed was sufficient to fracture the pellet. We surmise that at the higher speed of 5 mm s^{-1}, the shorter time of removal would not be responsible for fracture, but instead fracture would occur due to the magnitude of the applied force.

At the removal speed of the bee, 0.76 mm s^{-1}, the peak force was 23 ± 7.8 mN, the lowest force for all measured removal speeds. Moreover, the average peak force at 0.76 mm s^{-1} is significantly different [26] from those at 2.5 and 5.0 mm s^{-1} ($p = 0.004$ for 0.76 and 2.5 mm s^{-1}, $p = 0.02$ for 0.76 and 5.0 mm s^{-1}). The average peak forces at 2.5 and 5 mm s^{-1} are not significantly different from one another ($p = 0.1$). Nevertheless, the low peak force at the biologically relevant removal speed suggests an adaptive benefit for pushing on pellets slowly.

Another factor that could influence the bee's choice of leg speed is the work required to remove the pellet. The average work done for each speed is shown in figure 4*b*. The only work values that are significantly different from one another are at removal speeds of 0.76 mm s^{-1} and 5.0 mm s^{-1} ($p =$

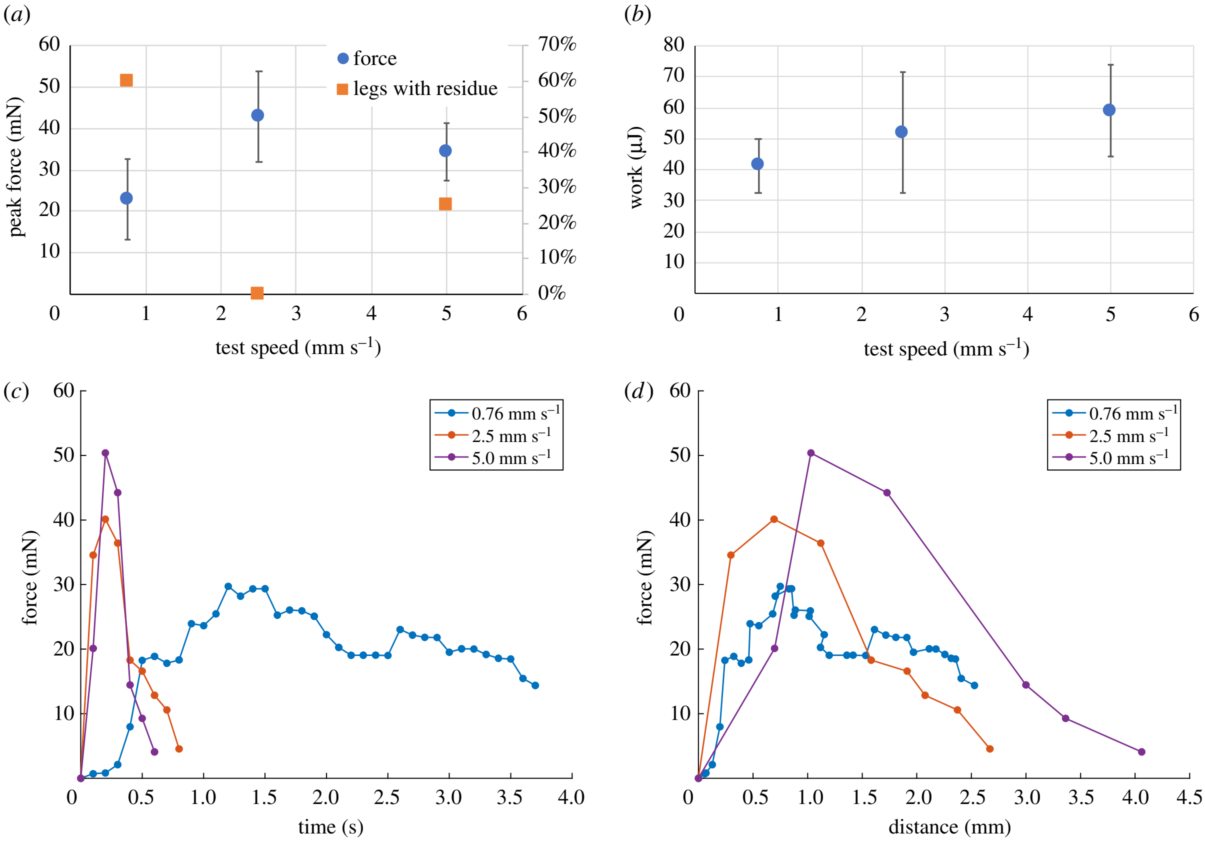

Figure 4. Force to remove the pollen pellet measured by automated pollen scraper. (*a*) Circles are the peak force at different speeds measured by the analytical balance in the pellet removal experiments. Bars on each data point are the 95% confidence intervals. Squares are the percentage of legs that had pollen residue left on them after the experiment was run at each speed. (*b*) The work done by the pellet removal experiments at different speeds. Bars on each data point are 95% confidence intervals. (*c*,*d*) Examples of force–time and force–distance relationships obtained by the analytical balance.

Table 1. The average measured peak pollen pellet removal force, the calculated work done at various removal speeds, and the number of legs that had pollen residue left on them after the experiment was completed. *N* is the number of trials at each speed.

speed of removal (mm s^{-1})	avg peak force ± s.d. (mN)	avg work done ± s.d. (µJ)	legs with residue	*N*
0.76	23 ± 7.8	41 ± 6.9	3	5
2.5	43 ± 6.9	52 ± 12	0	4
5.0	34 ± 13	59 ± 28	4	16

0.04). The average work done at 0.76 and 2.5 mm s^{-1} have $p = 0.23$, and at 2.5 and 5.0 mm s^{-1} have $p = 0.5$. The work done is 1.3 times greater at 5 mm s^{-1} than at the bee's speed of 0.76 mm s^{-1}. Together, these results suggest that the bee's choice of slow speed reduces applied force and expended energy compared with higher speeds. However, our leg scraper measurements do not give us a precise mechanism for how the pellet's material properties reduce the bee's energy use. To quantify the material properties, we turn to more controlled experiments with the pollen pellet alone.

3.3. Viscoelastic properties of the pollen pellet

In this section, we measure the behaviour of the pollen pellet under normal, compressive stresses using a UTM. Figure 6*a–c* and table 2 show Young's modulus, E, the viscosity, η and the relaxation time, $t_R = \eta/E$, of the pollen pellets, obtained from creep tests with approach speeds of 0.1 ($N = 8$), 0.5 ($N = 6$), 1 ($N = 9$) and 2 ($N = 2$) mm s^{-1}. The average stress–strain curves for the UTM creep experiments for all four speeds are shown in electronic supplementary material, figure S4.

The average Young's modulus E ranges from 43 to 95 kPa, which is comparable to the modulus of certain hydrogels [27,28], human muscles [27], and mucus and blood [28]. Because only two datasets were taken for an approach speed of 2 mm s^{-1}, a normal distribution cannot be assumed, and the significance of those results cannot be compared to the other averages [26]. The only average value of E that is significantly different is that of 0.5 and 1 mm s^{-1} ($p = 0.04$). The trend shows a slight decrease in E with increasing speed, which is unexpected for viscoelastic materials [29].

As shown in figure 6*b*, the viscosity increases as the test speed increases from 0.1 to 1 mm s^{-1} ($p = 0.01$). The increasing η with test speed outweighs the decreasing E, resulting in a relaxation time, $t_R = \eta/E$, that increases with test speed. The relaxation time is a measure for how long it takes for the applied stress to relax [23], or in other words, how long it takes for the viscous material response to dominate. Interestingly, the relaxation times shown in figure 6*c* at each speed are of the order of minutes. This is much longer than the timescales of the bee's pellet removal, our automated pellet removal and the pollen creep experiments. This suggests that the pollen pellet behaves effectively as a solid during the entire removal process. This is advantageous for the

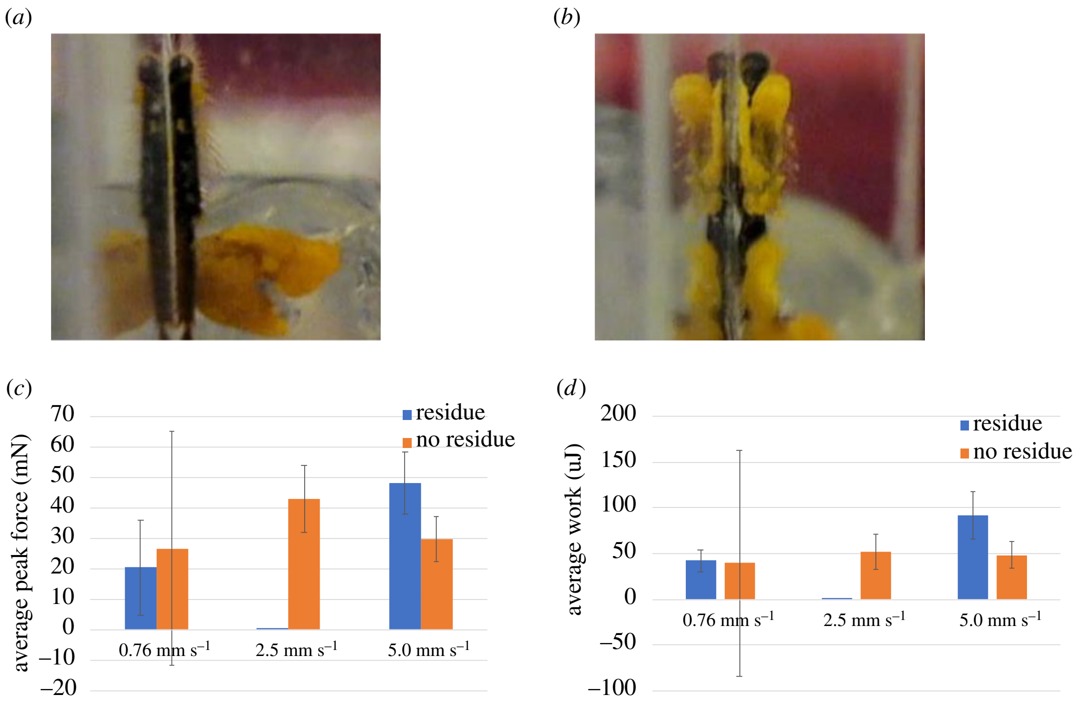

Figure 5. Pollen residue after pellet removal. Example of a removal with (*a*) no pollen residue and (*b*) residue left on the leg. (*c*) Average peak forces and (*d*) average work done for removal trials, with and without pollen residue. Bars shown are 95% confidence intervals.

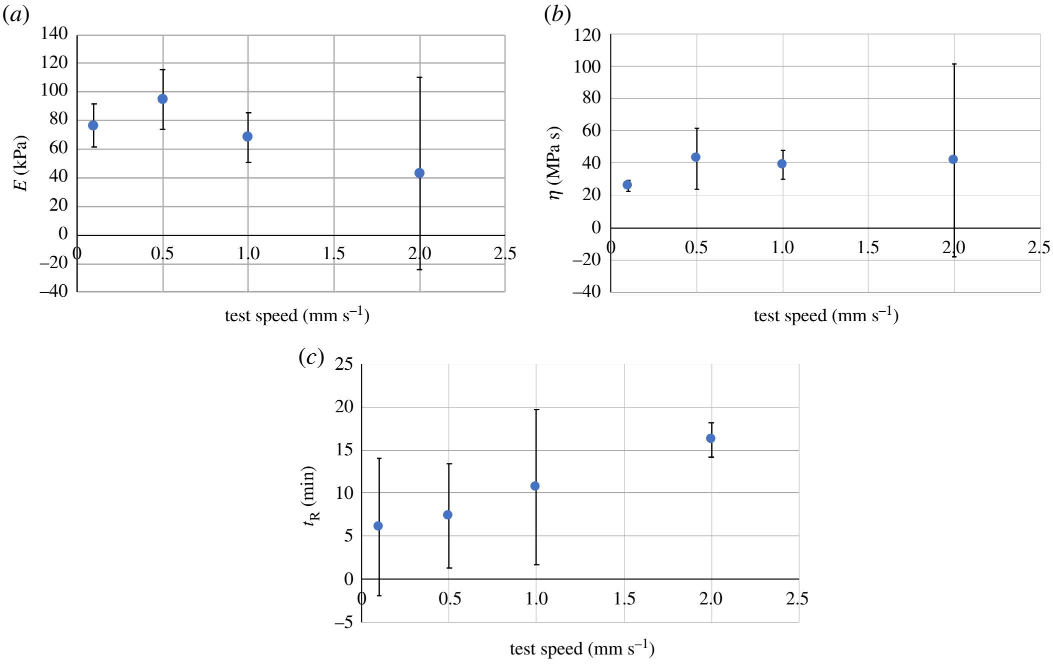

Figure 6. Viscoelastic properties of the pollen pellet. (*a*) Young's modulus E found for the pollen pellet based on creep tests on the UTM at different approach speeds. (*b*) The viscosity η found for the pollen pellet based on creep tests on the UTM at different approach speeds. (*c*) The relaxation time $t_R = \eta/E$ of the pollen pellets at different approach speeds.

honey bee because it will not lose its pollen load during flight due to the pellet flowing off.

4. Discussion

One of the key contributions of our study was the automated pollen scraper. Our device does not mimic the saw-like movement applied by the honey bee, nor does the smooth device mimic the hairy bee's leg. Nevertheless, our experiment still shows the response of the pollen pellet to removal at different speeds. Within the context of material behaviour, the pollen pellet's long relaxation time means there is no difference between one linear movement and many oscillating movements as neither exceeds that relaxation time in duration.

For context on the magnitude of the removal force, we note that the average worker honey bee has an average mass [30] of 116 ± 19 mg, so the honey bee's pellet removal force is 19 times greater than its body's gravitational force. It is known that bees, ants and other small insects can

Table 2. The measured Young's modulus, E, viscosity, η and the relaxation time, t_R with standard deviations. N is the number of trials at each speed.

approach speed (mm s^{-1})	avg $E \pm$ s.d. (kPa)	avg $\eta \pm$ s.d. (MPa s)	avg $t_R \pm$ s.d. (min)	N
0.1	77 ± 18	26 ± 4.4	6.1 ± 2.4	8
0.5	95 ± 20	43 ± 18	7.4 ± 2.3	6
1	68 ± 23	39 ± 11	11 ± 5.4	9
2	43 ± 7.5	42 ± 6.7	16 ± 0.24	2

apply large forces for their body weight [31,32], but the force we predict for bees may be at the upper limits of what bees can produce.

The large attachment force to the leg also indicates that the pellet is well secured during flight. A honey bee's entire body experiences a drag force of 1.15 mN while flying at 12 m s^{-1} [33]. The drag on the pellet is an order of magnitude smaller because of its smaller surface area. Thus the drag force during flight is unlikely to remove the pellet.

The pellet removal data in figure 4*c*,*d* and electronic supplementary material, figures S1–S3 show that while removing the pellet at any speed, the largest force occurs at the beginning of the removal process, and then the force quickly drops. In the videos of honey bees removing pellets in the hive, the overall leg movement in the y-direction (downwards) is slower in the first part of the removal, and then at 1.3 s in figure 2*d* the leg begins to move more quickly. Likewise, in a removal video in which the angle was not sufficient to track the fine movement of the middle leg (electronic supplementary material, video S3), the leg's overall speed in the y-direction is much slower in the beginning than at the end of the removal as shown in electronic supplementary material, figure 5. As described in §1, the hairs fringing the corbicula become embedded into the pellet. As the bee removes the pellet, more and more hairs are removed from the pellet as can be seen in figure 3*b*. From these observations, we surmise that these hairs are the main source of the adhesion force between the corbicula and the pellet. It appears that once enough hairs have been extracted from the pellet, the required force to remove the pellet drops significantly.

The instances of pollen residue being left on the bee leg during our automated pollen scraper experiments stands out against our observations of live bees in the hive. There are a few possible explanations for this. One is the increase in leg speed observed in real bees and the possible extraction of corbicular hairs, as discussed above. Our apparatus did not mimic this change in speed. Another explanation is that the linear movement of the removal arm in our experiment is not as effective as the oscillatory movement in honey bees. The oscillatory movement may allow more fine control and feedback to ensure that all pollen is removed.

Finally, there is a difference in geometry. The automated pollen scraper uses a removal arm that is six times smaller in diameter than a honey bee leg, has no hair, and is much more rigid than the honey bee leg. The scraper was chosen due to the inherent challenges with designing a repeatable experiment, as discussed in §2.3. It is possible that these differences are at least partially responsible for the fracture we observed and so are a possible area for future study.

It is unknown why the honey bee uses an oscillatory movement rather than a linear movement to remove pollen pellets. One possibility is that this oscillation is a more natural movement for a bee. It is also possible that reaching the required push off force is too difficult or impossible for the bee to do in one burst. Instead, the successive pushes may require less peak force while still accomplishing the goal of removing the pellet. While many studies have investigated the muscle mechanics and capabilities of honey bee wing muscles [34,35], the maximum force that can be exerted by their legs has not yet been investigated. Future work could imitate the oscillating movement of the bee leg to discover any differences in force and work to remove the pellet, as well as understand its impact in fracturing the pellet.

Another difference between the automated pollen scraper and the honey bee is the geometry of the scraping element. In the bee, the legs are very close and possibly in contact with each other during the pellet removal process. In our apparatus, the scraper is as close as we could make it without getting stuck on the top of the leg or touching the corbicula directly. Such a safety factor was needed because our apparatus runs in open loop. In comparison, the bee's highly articulate and sensitive scraping leg permits it to get very close to the pellet. Our videos captured the linear and oscillatory speed, but not any subtle changes in angle or direction. It is possible the bee peels or rolls the pellet off of the corbicula in ways that the automated pollen scraper cannot imitate. These differences in motion may affect the removal force.

The material property measurements showed that Young's modulus of the pellet changed only slightly with speed of stress application within the speed range we tested. The lowest relaxation time of the pellet was 6.1 min at a test speed of 0.1 mm s^{-1}, which is much slower than the bee's pellet removal speed U. This relaxation time was 140 times longer than the time a bee takes to remove its pellets, $T = 2.6$ s, which means the pellet acted like an elastic solid during removal. Our results showed that Young's modulus does not change much with the speed of removal. Therefore, the measured viscoelastic material properties cannot explain the results we found with the automated pollen scraper, that peak removal force increases with increasing removal speed. However, neither the UTM tests nor the automated pollen scraper experiments imitate the exact removal geometry and dynamics of the bee. Future studies could investigate the behaviour of the pollen pellet under stress from different directions. They could also use adhesion tests with varying approach speeds to measure the pollen pellet's adhesion energy with the corbicula, such as with an AFM. Such techniques have previously been used for measuring pollen adhesion [36–38].

An important difference in the removal and UTM experiments is the nature of the applied stress. When our automated scraper removes pellets, the pellet undergoes shear. By contrast, the pellets in our UTM experiments only underwent normal, compressive stress. However, the bee uses a combination of these two processes. The difference in stress type could lead to differences in the behaviour of the pellets. Moreover, the Maxwell model is valid for small deformations, but as shown in electronic supplementary material, video S1, the pollen pellet goes through large plastic deformation in the automated pollen scraper experiments. This large deformation does not occur in the natural removal process, so the behaviour of the pellet under small deformations is relevant to the biological process.

In this study, we did not control for type of pollen or nectar because doing so would require manipulations such as moving the entire hive to an area with only a single type of pollen available. Honey bees are polylectics, or generalists, meaning they will collect pollen from a wide variety of plant species [39,40]. Pollen can vary in size [41] between 7 and 617 µm, although most species have grains that are between 20 and 40 µm in size [42], as well as surface structure, having either smooth, grooved (reticulate) or very spiky (echinate) surfaces [43]. Nectar can vary in sugar concentration and other constituents [44]. Thus, it is possible that differences in pollen and nectar type could lead to different removal forces and pellet behaviour.

5. Conclusion

The results presented in this paper glean insight into how honey bees optimize their motion in order to efficiently remove pollen pellets in the hive. We developed a new method for close observation of honey bees removing pollen pellets in the hive, a process that had not been studied in detail before. We designed and built a new apparatus for measuring the force to remove pollen pellets at various speeds. We applied methods from soft-matter physics to measure the mechanical properties of the pellet. Our results suggest that the honey bees remove pollen pellets at a speed that reduces the force and work required. We have also shown that pollen pellets, a mixture of pollen and nectar, are viscoelastic, but the relaxation time is long enough to ensure that the pellets will exhibit primarily elastic behaviour during removal. These results can also inform the design of systems in which both the adhesion of soft matter to a substrate and its easy removal are desired.

Data accessibility. All data for this study can be found in the electronic supplementary material files.

Authors' contributions. M.M. conceptualized the study, designed and conducted experiments, analysed data, and wrote original draft. C.D.E., O.H. and O.L. designed and conducted experiments, analysed data and edited the manuscript. G.S. analysed and interpreted data and edited the manuscript. P.Y. interpreted data and edited the manuscript. D.H. conceptualized and supervised the study, interpreted data and edited the manuscript.

Competing interests. We declare we have no competing interests.

Funding. Research reported in this publication was supported in part by the Georgia Institute of Technology President's Undergraduate Research Award (PURA). Its contents are solely the responsibility of the authors and do not necessarily represent the official views of the Georgia Institute of Technology. This work was funded in part by the US Department of Agriculture, National Institute of Food and Agriculture grant no. 2016-67032-24986. This material is based upon work supported by the National Science Foundation Graduate Research Fellowship (grant no. DGE-1650044).

Acknowledgements. Dr J. Leavey and the Georgia Tech Urban Honey Bee Project made this work possible by maintaining Georgia Tech's apiary and being an excellent source of honey bee biology knowledge. Thanks to Dr S. Bhamla for letting us use his Dun, Inc. imaging system, and to X. Xu for helping us take the images. We are thankful to S. Puvvada, X. Li and K. Archer for their early contributions.

References

1. Kier WM, Smith AM. 2002 The structure and adhesive mechanism of octopus suckers. *Integr. Comp. Biol.* **42**, 1146–1153. (doi:10.1093/icb/42.6.1146)
2. Federle W, Riehle M, Curtis ASG, Full RJ. 2002 An integrative study of insect adhesion: mechanics and wet adhesion of pretarsal pads in ants. *Integr. Comp. Biol.* **42**, 1100–1106. (doi:10.1093/icb/42.6.1100)
3. Chen S, Gao H. 2007 Bio-inspired mechanics of reversible adhesion: orientation-dependent adhesion strength for non-slipping adhesive contact with transversely isotropic elastic materials. *J. Mech. Phys. Solids* **55**, 1001–1015. (doi:10.1016/j.jmps.2006.10.008)
4. Gorb SN. 2008 Biological attachment devices: exploring nature's diversity for biomimetics. *Phil. Trans. R. Soc. A* **366**, 1557–1574. (doi:10.1098/rsta.2007.2172)
5. Ewoldt RH, Winegard TM, Fudge DS. 2011 Non-linear viscoelasticity of hagfish slime. *Int. J. Non-Linear Mech.* **46**, 627–636. (doi:10.1016/j.ijnonlinmec.2010.10.003)
6. Chaudhary G, Ewoldt RH, Thiffeault J-L. 2019 Unravelling hagfish slime. *J. R. Soc. Interface* **16**, 20180710. (doi:10.1098/rsif.2018.0710)
7. Ewoldt RH, Hosoi AE, McKinley GH. 2009 Nonlinear viscoelastic biomaterials: meaningful characterization and engineering inspiration. *Integr. Comp. Biol.* **49**, 40–50. (doi:10.1093/icb/icp010)
8. Lakes R, Lakes RS. 2009 *Viscoelastic materials*. New York, NY: Cambridge University Press.
9. Klein A-M, Vaissière BE, Cane JH, Steffan-Dewenter I, Cunningham SA, Kremen C, Tscharntke T. 2007 Importance of pollinators in changing landscapes for world crops. *Proc. R. Soc. B* **274**, 303–313. (doi:10.1098/rspb.2006.3721)
10. Brodschneider R, Crailsheim K. 2010 Nutrition and health in honey bees. *Apidologie* **41**, 278–294. (doi:10.1051/apido/2010012)
11. García-García MC, Ortiz PL, Dapena MJD. 2004 Variations in the weights of pollen loads collected byapis melliferal. *Grana* **43**, 183–192. (doi:10.1080/00173130410020350)
12. Milne Jr CP, Pries KJ. 1984 Honeybee corbicular size and honey production. *J. Apic. Res.* **23**, 11–14. (doi:10.1080/00218839.1984.11100601)
13. Ford DM, Hepburn HR, Moseley FB, Rigby RJ. 1981 Displacement sensors in the honeybee pollen basket. *J. Insect. Physiol.* **27**, 339–346. (doi:10.1016/0022-1910(81)90080-9)
14. Hodges D. 1967 The function of the 'single hair' on the floor of the honeybee's corbicula. *Bee World* **48**, 58–62. (doi:10.1080/0005772X.1967.11097144)
15. Casteel DB. 1912 The behavior of the honey bee in pollen collecting. *USDA Bureau Entomol. Bull.* **121**, 13–18.
16. Michener CD, Winston ML, Jander R. 1978 Pollen manipulation and related activities and structures in bees of the family apidae. *Univ. Kansas Sci. Bull.* **51**, 575–601. (doi:10.5962/bhl.part.17249)
17. Dreller C, Tarpy DR. 2000 Perception of the pollen need by foragers in a honeybee colony. *Anim. Behav.* **59**, 91–96. (doi:10.1006/anbe.1999.1303)
18. Seeley TD. 1996 *The wisdom of the hive: the social physiology of honey bee colonies*. Cambridge, MA: Harvard University Press.
19. von Frisch K, von Frisch O, Gombrich L. 1974 *Animal architecture*. New York, NY: Harcourt Brace Jovanovich.
20. Willingham R, Klopchin J, Ellis J. 2018 Robbing behavior in honey bees. Technical Report ENY-163, Gainesville, FL: University of Florida Institute of Food and Agricultural Sciences.

21. Snodgrass RE. 1984 *Anatomy of the honey bee*. Ithaca, NY: Cornell University Press.
22. Guillermo JA, Marguerite M, D'Andre W, Megha M, Stanislav NG, David LH. 2017 Honey bee hairs and pollenkitt are essential for pollen capture and removal. *Bioinspir. Biomim.* **12**, 026015. (doi:10.1088/1748-3190/aa5c6e)
23. Kelly PA. 2013 *Mechanics lecture notes: an introduction to solid mechanics*. Auckland, New Zealand: The University of Auckland.
24. Roeder RK. 2013 Chapter 3. Mechanical characterization of biomaterials. In *Characterization of biomaterials* (eds A Bandyopadhyay, S Bose), pp. 49–104. Oxford, UK: Academic Press.
25. Rabelo JMG, Becho JS, Greco M, Cimini Jr CA. 2018 Modeling the creep behavior of grfp truss structures with positional finite element method. *Latin Am. J. Solids Struct.* **15**, 3.
26. Fay DS, Gerow K. 2013 A biologist's guide to statistical thinking and analysis. In *WormBook* (ed. The *C. elegans* Research Community). (doi:10.1895/wormbook.1.159.1)
27. Liu J, Zheng H, Poh PSP, Machens H-G, Schilling AF. 2015 Hydrogels for engineering of perfusable vascular networks. *Int. J. Mol. Sci.* **16**, 15997–16016. (doi:10.3390/ijms160715997)
28. Zhao H, Xu K, Zhu P, Wang C, Chi Q. 2019 Smart hydrogels with high tunability of stiffness as a biomimetic cell carrier. *Cell Biol. Int.* **43**, 84–97. (doi:10.1002/cbin.11091)
29. Tirella A, Mattei G, Ahluwalia A. 2014 Strain rate viscoelastic analysis of soft and highly hydrated biomaterials. *J. Biomed. Mater. Res. A* **102**, 3352–3360. (doi:10.1002/jbm.a.34914)
30. Zółtowska K, Fraczek R, Lipinski Z. 2011 Hydrolases of developing worker brood and newly emerged worker of *Apis mellifera carnica*. *J. Apic. Sci.* **51**, 27–37.
31. Alexander RM. 1985 The maximum forces exerted by animals. *J. Exp. Biol.* **115**, 231–238. (doi:10.1242/jeb.115.1.231)
32. Phonekeo S, Dave T, Kern M, Franklin SV, Hu DL. 2016 Ant aggregations self-heal to compensate for the Ringelmann effect. *Soft Matter* **12**, 4214–4220. (doi:10.1039/C6SM00063K)
33. Nachtigall W, Hanauer-Thieser U. 1992 Flight of the honeybee. *J. Comp. Physiol. B* **162**, 267–277. (doi:10.1007/BF00357534)
34. Altshuler DL, Dickson WB, Vance JT, Roberts SP, Dickinson MH. 2005 Short-amplitude high-frequency wing strokes determine the aerodynamics of honeybee flight. *Proc. Natl Acad. Sci. USA* **102**, 18 213–18 218. (doi:10.1073/pnas.0506590102)
35. Sun M. 2014 Insect flight dynamics: stability and control. *Rev. Mod. Phys.* **86**, 615–646. (doi:10.1103/RevModPhys.86.615)
36. Ito S, Gorb SN. 2019 Fresh 'pollen adhesive' weakens humidity-dependent pollen adhesion. *ACS Appl. Mater. Interfaces* **11**, 24 691–24 698. (doi:10.1021/acsami.9b04817)
37. Ito S, Gorb SN. 2019 Attachment-based mechanisms underlying capture and release of pollen grains. *J. R. Soc. Interface* **16**, 20190269. (doi:10.1098/rsif.2019.0269)
38. Shin D, Choi WT, Lin H, Qu Z, Breedveld V, Meredith JC. 2019 Humidity-tolerant rate-dependent capillary viscous adhesion of bee-collected pollen fluids. *Nat. Commun.* **10**, 1379. (doi:10.1038/s41467-019-09372-x)
39. Vanderplanck M, Moerman R, Rasmont P, Lognay G, Wathelet B, Wattiez R, Michez D. 2014 How does pollen chemistry impact development and feeding behaviour of polylectic bees? *PLoS ONE* **9**, e86209. (doi:10.1371/journal.pone.0086209)
40. Ritchie AD, Ruppel R, Jha S. 2016 Generalist behavior describes pollen foraging for perceived oligolectic and polylectic bees. *Environ. Entomol.* **45**, 909–919. (doi:10.1093/ee/nvw032)
41. Knight CA, Clancy RB, Götzenberger L, Dann L, Beaulieu JM. 2010 On the relationship between pollen size and genome size. *J. Bot.* **2010**, 1–7.
42. Muller J. 1979 Form and function in angiosperm pollen. *Annals of the Missouri Botanical Garden* **66**, 593–632. (doi:10.2307/2398913)
43. Lin H, Gomez I, Meredith JC. 2013 Pollenkitt wetting mechanism enables species-specific tunable pollen adhesion. *Langmuir* **29**, 3012–23. (doi:10.1021/la305144z)
44. Nicolson SW, Nepi M, Pacini E. 2007 *Nectaries and nectar*, vol. 4. Berlin, Germany: Springer.